Cureus Journal of Computer Science

Open Access Original Article

# Effective Multiclass Grapevine Leaves Disease Classification Using Hyperspectral Imaging and Optimized Artificial Neural Network

**Received** 05/01/2025
**Review began** 05/23/2025
**Review ended** 06/14/2025
**Published** 07/01/2025



**DOI:** https://doi.org/10.7759/s44389-025-05883-5

Jyotisana Meena [1] , Sujatha Narayanan Unni [1]

1. Applied Mechanics and Biomedical Engineering, IIT Madras, Chennai, IND

**Corresponding author:** Sujatha Narayanan Unni, nsujatha@iitm.ac.in

## Abstract

Grapevine farming is one of the most common and economical agricultural practices worldwide. The grapevine crop is affected by various diseases caused by biotic or abiotic stress, which degrade production and quality. Therefore, precise identification of disease is predominant for sustainable viticulture. This article proposes a potential solution for automatically detecting various diseases, damages, and healthy samples. The study develops an optimized artificial neural network (ANN) and trains it with a composite loss function consisting of weighted categorical cross-entropy (WCCE) and label smoothing (LS). The WCCE helps address the class imbalance challenge, whereas LS prevents the model from being overconfident and makes it generalized. The study utilizes the grapevine leaf hyperspectral imaging dataset, which falls under the visible and near infrared (400-900 nm) range and has 204 bands/wavelengths from 87,305 spectra extracted via the region of interest. The 30 signature relevant wavelengths for disease detection, identified using linear discriminant analysis, are significant as they represent the most informative parts of the spectrum for disease detection, thereby helping reduce data redundancy. For further experimentation, the dataset was randomly split into Dataset-A, which contained 70% of the total spectra for a 10-fold cross-validation setting, and the remaining 30% was allocated to Dataset-B, which was reserved as an unseen dataset to evaluate the model's robustness. The optimized ANN performed best among the other classifiers in terms of performance metrics (classification accuracy, precision, recall, and F1-score). For the full range, the optimized ANN achieved 96.37%±0.26% classification accuracy on Dataset-A and 96.47% on Dataset-B. Moreover, for the significant 30 wavelengths, the optimized ANN achieved 95.47%±0.34% classification accuracy on Dataset-A and 95.17% classification accuracy on Dataset-B. The promising results demonstrated that the proposed model can be used as a mass-screening tool for potential diseases to boost the production and quality of the grape crop.

**Categories:** AI applications, Big Data and Analytics, Machine Learning (ML)
**Keywords:** non-destructive, multiclass classification, optimized artificial neural network, random forest, k-nearest neighbor, grapevine leaves., hyperspectral imaging

## Introduction

The increasing global population's shift toward healthier diets has driven demand for high-quality grape production [1]. However, grapevine diseases threaten food security by causing significant yield losses [2]. There is a strong need for qualitative production to meet this demand and address these challenges. In this regard, innovative and precision agriculture is crucial to supporting farmers in optimizing their outcomes within modernised agriculture [1]. Grapevine farming is one of the most common and economical agricultural practices worldwide [1,3]. Vine production plays a significant role in agriculture due to its contributions to culinary arts [1] and its positive impact on economic development through the production of wine as well as fresh fruit and raisins [1,3]; therefore, maintaining vine health is essential for sustainable viticulture [2]. However, vine farming faces several challenges affecting both farmers and consumers, including unpredictable weather conditions, pests, limited resources, and various grapevine diseases [1].

Grapevine disease worldwide causes significant economic losses annually. The pathogens infect vines primarily through pruning wounds in the field but can also be found in nurseries; thus, dissemination through newly grafted vines cannot be excluded [4]. Grapevines are affected by various diseases, especially those impacting the leaves [3], including downy mildew, spider mites, black rot, black measles, leaf blight, grapevine leafroll disease (GLD), grapevine red blotch (GRB), grapevine yellows, etc. [2]. The most common diseases in grapevines worldwide are black rot, mold, flavescence dorée (a specific grapevine yellow disease), Esca (a highly harmful grapevine trunk disease), downy mildew, GLD, etc., caused by various infections such as bacteria, viruses, nematodes, and parasites [1]. In some complex diseases like Esca, external symptoms are not visible until several years after infection, which can lead to the death of the infected vines [4]. Powdery mildew and red blotch are the most common diseases that significantly challenge grape growers. Powdery mildew is the most frequently found and dangerous fungal disease among others, appearing as white powdery growth on leaves, disrupting photosynthesis and weakening

**How to cite this article**
Meena J, Narayanan Unni S (July 01, 2025) Effective Multiclass Grapevine Leaves Disease Classification Using Hyperspectral Imaging and Optimized Artificial Neural Network . Cureus J Comput Sci 2 : es44389-025-05883-5. DOI https://doi.org/10.7759/s44389-025-05883-5

the plant [3]. One study involving concord grapes revealed that powdery mildew reduces the fruit's sugar levels, juice colour, and acidity [5]. GRB disease is caused by viruses and appears as yellowing of leaves, reducing chlorophyll production and nutrient absorption [3].

The significant challenges lie in the similarity of disease symptoms, which can confound accurate identification of the specific problem, which is particularly common in grapevine diseases. For instance, the symptoms of GLD are caused by the grapevine leafroll-associated virus (GLRaV), and the initial stages of infection are evident as red discolouration in grapevine leaves [6]. Similar symptoms are easily mistaken for GRB disease, resulting from grapevine red blotch virus, which induces red blotch signs on the leaves, particularly along the prominent veins, varying with grapevine variety. Discrimination of these red discolourations is essential for accurately identifying the causing agent. Symptoms from grapevine leafroll-associated virus and grapevine red blotch virus usually co-occur in the same vineyard and plant [2]. However, different grapevine cultivars differ in their sensitivity based on disease complexity. No cultivated or wild grapevine species is disease-resistant [4]. So far, the correlation between the severity of the disease and the expression of the leaf symptoms has not been shown since, based on the appearance of the leaves, the disease severity cannot be predicted from year to year. In commercial vineyards, precise disease diagnosis is crucial for identifying and quantifying the pathogen, guiding effective disease management [3]. Therefore, annual monitoring is essential to estimate the disease incidence in vineyards [4]. The only treatment for these diseases is pesticide use, which harms humans and the environment [2]. Therefore, for the limitation of pesticides, precise disease identification and timely disease diagnosis require a strong management strategy for healthy production and sustainability of grapevine crops [2,3].

Traditional methods like expert advice, visual inspection, and laboratory tests for diagnosing grapevine disease are subjective, time-consuming, costly, error-prone, and labour-intensive and have less potential in precision agriculture [1,2,4]. Furthermore, these methods are not feasible in large grapevine fields due to the high labour-intensive survey requirement [3]. Therefore, there is a high demand for fast, accurate, cost-effective, and reliable automated approaches to detecting and classifying grapevine leaf disease and overcoming these challenges [7].

Experts such as horticulture scientists and pathologists have utilised numerous modern imaging techniques to identify plant irregularities and disease diagnosis, including Digital Imaging, Spectrometry, Hyperspectral Imaging (HSI), Multispectral Imaging (MSI), Thermal Imaging, Fluorescence Imaging, X-ray Imaging, and Ultraviolet Imaging [2]. Among these techniques, HSI and MSI are the most popular optical technologies and provide a non-invasive and objective assessment of diseases of various kinds of plants in the whole field. These techniques offer better analysis and information content based on the biochemical and biophysical changes in the plants for visible (VIS) to shortwave infrared (SWIR) range, for the whole spectrum (HSI) or the selected bands (MSI), unlike RGB imaging [4]. Recently, the HSI has been widely used for various symptomatic and asymptomatic grapevine diseases such as powdery and downy mildew, GLD, grapevine yellows, and foliar Esca symptoms in grapevine trunk disease, etc. [4]. The HSI technique provides detailed information about plants' spectral and spatial characteristics, which can be utilised for disease detection [2].

Advancements in technology, especially in artificial intelligence (AI), machine learning (ML), and deep learning (DL), provide prominent solutions and have positively impacted various agricultural applications such as crop management, water management, soil management, and livestock management [2]. These techniques can give grapevine disease management and effective and accurate disease detection, allow for early intervention before deterioration, reduce disease spread, and minimise yield losses [3]. The ML models were used in grapevine agriculture to improve health, production, sustainability, and economic viability while reducing pesticide use [2]. DL has also garnered attention recently for its potential to revolutionise grapevine disease detection [2]. The use of AI tools to analyse grapevine data has changed grapevine research rapidly in the past few years [1]. Furthermore, adopting AI-driven solutions in agriculture can lead to more accurate and data-driven employment practices and drive innovative and technological improvements in the industry [7].

Incorporating optical imaging techniques and AI could facilitate a streamlined and cost-effective solution to transform the landscape of plant disease detection [2]. HSI and MSI with ML have emerged as promising techniques for detecting various plant diseases and have also become a significant approach in smart agriculture [1]. The involvement of MSI and HSI techniques with technological evolution AI has improved and progressed to increase the detection of mild and moderate symptoms of these adverse diseases, such as powdery mildew and red blotch [8]. It is worth pointing out that HSI can detect disease early before the symptoms are observable, thereby ensuring proactive prevention and treatment [8]. These technological innovations' integration with HSI may present a more focused and better solution for disease detection, limited pesticide use, lessening environmental harm, less intensive labour, and prolonged processes, and becoming more reliable and achievable for farmers and agricultural practitioners [2,8].

The current research aims to develop a robust AI-based multiclass classification model (MCC) to detect various diseases and damage in grapevine leaves automatically. The study proposed an approach to manage diseases' impact on grapevine crops, alleviate wastage and cost, and reduce the excessive use of pesticides, which have adverse environmental effects. The study also highlights the significance of the most relevant wavelengths for predicting the outcomes using the proposed model.

The main contributions of this research are as follows:

1. A novel AI-based multi-classification model for classifying disease, damaged, and healthy leaves in imbalanced grapevine leaves HSI data samples with the best reported accuracy.

2. Reduction in data redundancy by incorporating the most significant wavelengths contributing to the leaves' classification using the linear discriminant analysis (LDA) technique.

3. The ANN model was optimised utilising the hybrid loss function comprising weighted categorical cross-entropy and label smoothing to address the class imbalance and hard predictions to boost generalisation.

4. An optimised ANN model outperformed other ML models employed for multi-class classification of damaged, diseased, and healthy grapevine leaves.

### Related work

Towards the same direction, recent research has been performed using the HSI system and various DL models on the investigation of different crops diseases such as citrus fungal disease detection [9], classification of grapevine images of healthy and diseased leaves with powdery mildew and Blotches disease [3], classification of grapevine leaves with asymptomatic and symptomatic leaves with Grapevine leaf stripe disease [10], and the classification of grapevine fruits and leaves samples (including downy mildew-diseased fruit, downy mildew diseased leaves, healthy leaves, powdery mildew diseased fruits, and powdery mildew diseased leaves) [11].

Furthermore, Knauer et al. [12] utilised a VIS-NIR HSI camera from a spectral range of 400-1000 nm with 3.7 nm spectral resolution and a total of 160 spectral bands and a SWIR HSI camera of 970-2500 nm spectral range with 6 nm spectral resolution and 256 total bands for the assessment of powdery mildew in vines. Their study analysed visually 10 healthy bunches and 20 bunches naturally infected with *Erysiphe necator*, including 10 infected and 10 severely diseased bunches of vines. Their study used a pixel-wise spectral classification method with a 10-fold cross-validation (CV) setting to classify healthy and infected grapes. It achieved 98% and 85% training accuracy for VIS-NIR and SWIR wavelength ranges, respectively. Gao et al. [6] utilised a line scan HSI system with a spectral range from 517 to 1729 nm with an 8.3 nm spectral resolution and 148 spectral bands, a conveyor belt, and a 150-W tungsten halogen lamp to illuminate samples. Their study analysed 500 grapevine leaf samples, including healthy and infected grapevine leaves, at five growth stages for three consecutive sessions in 2017, 2018, and 2019, respectively, for the non-destructive detection of GLD. The study used the least absolute shrinkage and selection method to select the six feature wavelengths and later used these six wavelengths for the least squares support vector machine classifier and achieved the classification accuracy of 66.67%, 76.55%, and 89.93% for the test dataset collected at the first asymptomatic stage for three seasons, respectively. Pérez-Roncal et al. [13] utilized a line scan HSI system with a spectral range from 900 to 1700 nm with 3.14 nm spectral resolution to collect the 74 grapevine leaves data, including healthy (24), asymptomatic (24), and symptomatic (24) leaves. Their study utilized partial least squares discriminant analysis to discriminatively between healthy, asymptomatic, and symptomatic leaves and achieved 82.78-95.53% accuracy for the full spectrum in the CV setting. Their study also highlights that the 1596-1687 nm range was most important for the three class classifications (healthy, asymptomatic, and symptomatic) while (1000-1029, 1126-1154, 1408-1436, 1534-1562, and 1659-1687 nm) were selected for healthy and asymptomatic classes differentiation. Lacotte et al. [14] utilized a Specim FX10 HSI camera with 400-1000 nm spectral ranges with 5.5 nm spectral resolution and 224 bands to acquire the hyperspectral images of grapevine leaves in the illumination of a halogen lamp. The dataset contains 1,386 patches from 62 leaves, including healthy leaf patches (771) and diseased leaf image patches (615) infected with downy mildew. They split the dataset into a training (80%) and a test dataset (20%). The training dataset contained 1,102 patches, including 665 normal patches and 437 diseased leaves. The test dataset contained 284 patches, including 106 normal and 178 infected leaves. Their study utilized a support vector machine classifier for classification based on the spatial and spectral database of infected and healthy leaf patches with a 10-fold CV setting. It obtained 96% classification accuracy on the validation and 99% on the test datasets.

The state-of-the-art (SOA) method reported in the literature utilised different AI models and imaging systems for disease classification in various crop samples. However, these methods can discriminate between healthy and diseased samples infected with a maximum of one or two kinds of disease. Therefore, there is a need for an effective multiple-disease detection method that contributes to crop health protection. There is still room for improvement in a more robust MCC model to distinguish similar disease symptoms from healthy samples.

## Materials And Methods

## Dataset sources and description

The HSI database of grapevine leaves was used for this study, which was sourced from the publicly available dataset by Ryckewaert et al. [15]. The dataset contains 205 HSI images with an equal ratio of red and white grapevine leaves. The leaves are from seven grapevine varieties, including damaged, healthy, and diseased leaves with foliar symptoms caused by ten different grapevine diseases. Foliar symptoms showed the symptoms of biotic and abiotic stress on the various parts of the leaves. The HSI images of grapevine leaves were acquired under controlled laboratory conditions in the proper illumination of a halogen lamp using the VIS-NIR Specim IQ hyperspectral camera, which has a spectral range from 400-900 nm, with a spectral resolution of 7 nm. Later, the dark and white reference correction was done for each HS image of the grapevine leaves using Equation 1.

$$R(\lambda) = \frac{I(\lambda) - I_d(\lambda)}{I_o(\lambda) - I_d(\lambda)} \qquad (1)$$

where $I(\lambda)$ is the intensity of reflected light, $I_d(\lambda)$ is the intensity of dark current, and $I_o(\lambda)$ is the intensity of standard reference.

For further analysis, the current study extracted a total of 87,035 spectra by selecting the region of interest on each leaf image using the Spectral Python (SPy) module. Total spectra include 3,873 damaged, 11,657 healthy, and 71,505 diseased spectra. The total number of leaves in each category (damaged, healthy, and diseased) and the corresponding extracted spectra for the particular category are reported in Table *1*.

| Leaves category | Number of classes | Symptoms | Number of leaves | Number of spectra |
|---|---|---|---|---|
| Damaged | 0 | Damage (hail, harvester) | 5 | 3,873 |
| Healthy | 1 | Healthy | 40 | 11,657 |
| Diseased | 2 | Flavescence dorée (*Scaphoideus titanus*) | 80 | 29,579 |
| | 3 | Green leafhopper (*Empoasca vitis*) | 20 | 8,597 |
| | 4 | Buffalo treehopper (*Stictocephala bisonia*) | 17 | 6,593 |
| | 5 | Wood diseases | 17 | 6,742 |
| | 6 | Water stress | 13 | 4,938 |
| | 7 | Senescence | 8 | 3,382 |
| | 8 | Downy mildew (*Plasmopara viticola*) | 2 | 4,651 |
| | 9 | Chlorosis | 1 | 3,223 |
| | 10 | Discoloration | 1 | 2,729 |
| | 11 | Deficiency | 1 | 1,071 |

**TABLE 1: Summary of grapevine hyperspectral imaging dataset utilised for the multiclass disease classification.**

Furthermore, we applied the Savitzky-Golay smoothing [16] data pre-treatment technique using a window size of 21 and a third-order polynomial to obtain the filtered reflectance spectra for all the leaves. Later, the total data (87,035 spectra) was randomly split into train and test sets for experimentation purposes. Dataset-A (60,924) contains 70% of the data for the 10-fold CV setting. The remaining 30% of data was assigned to Dataset-B (26,110), which was exclusively used as an unseen dataset to test the model's robustness. The distribution of data among the different classes of the grapevine leaves for the multi-class classification task is shown in Figure *1*.

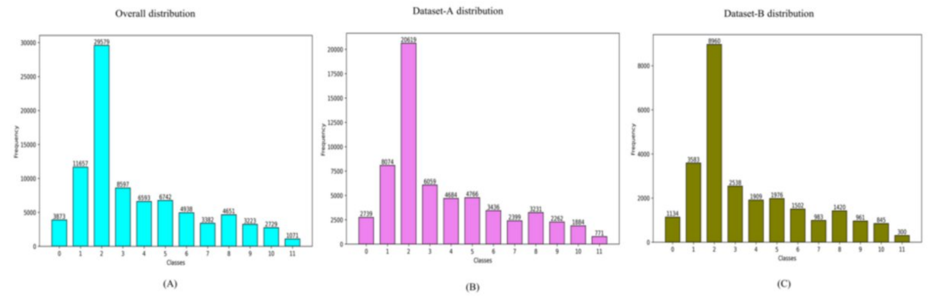


**FIGURE 1: Visualisation of the distribution of the spectra in each class for the grapevine dataset.**

## Proposed methodology for leaves classification: MCC

The proposed study developed three MCC models on the publicly available grapevine leaves dataset using three classifiers: Optimised ANN [17], K-Nearest Neighbor (KNN) [18], and Random Forest Classifier (RFC) [19]. The study compared the performance of each classifier for grapevine leaves classification, including damaged, healthy, and t10 kinds of diseased leaves with biotic or abiotic stress. The data used for the experiment is randomised with a random state parameter to ensure consistency. Furthermore, the signature wavelengths were estimated using LDA [20]. The technique helped to identify 30 selective wavelengths relevant for leaf classification purposes. The models were experimented with on Dataset-A under a 10-fold CV setting, and later the best-performing model was saved for further experimentation with unseen Dataset-B. Figure 2 illustrates the graphic overview of the proposed methods.

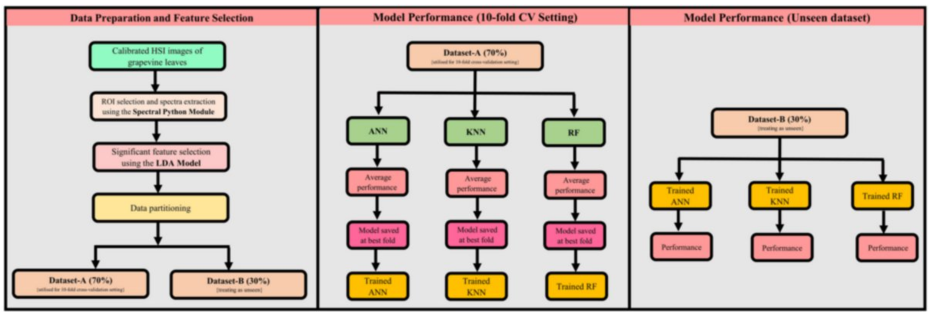


**FIGURE 2: Grapevine leave classification models overview.**

HSI, Hyperspectral Imaging; LDA, Linear Discriminant Analysis; CV, Cross-Validation; ANN, Artificial Neural Network; KNN, K-Nearest Neighbors; RF, Random Forest

*Development of an Optimised ANN Model*

ANN is a computational ML method inspired by biological neural networks (NN), which was developed by mimicking the human brain. ANN is an interconnection of nodes similar to neurons. The representative optimised ANN model used for this study is shown in Figure 3.

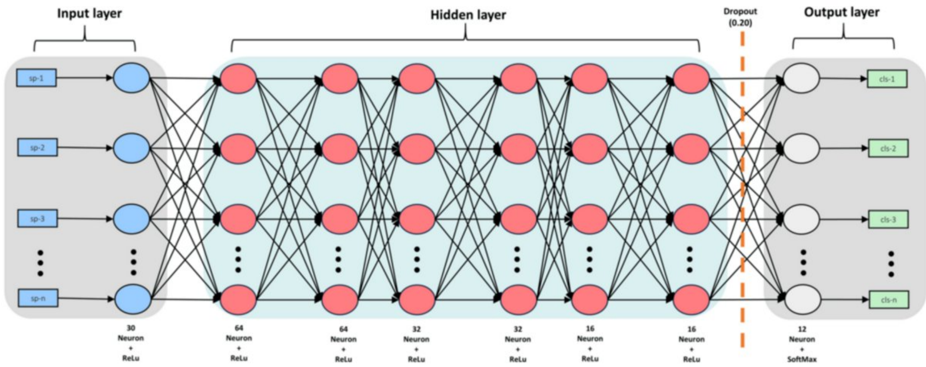


**FIGURE 3: Proposed optimised ANN model architecture.**

ANN, Artificial Neural Network; sp: Spectrum, cls: Classes

The hyperparameters selected for training and optimising the ANN are reported in Table 2.

| Hyperparameters | Details |
|---|---|
| Epochs | 2,000 |
| Batch size | 1,000 |
| Learning rate | 0.001 |
| Optimiser | Adam |
| Loss function | Weighted categorial cross-entropy + label smoothing (smoothing factor = 0.25) |

**TABLE 2: Hyperparameters utilised in an optimised ANN model.**

ANN, Artificial Neural Network

To develop the optimised ANN model, we implemented a composite loss function incorporating weighted categorical cross-entropy with label smoothing (LS) [21]. This composite loss function deals with the class imbalance challenge and increases the model's ability to manage uncertain and ambiguous predictions. The LS is an effective regularisation tool, which generates soft labels and provides strong regularisation for a learnable classification model. LS prevents the learned models from becoming overconfident, improving the classification performance and generalisation; conversely, class weighting compensates for uneven class distributions. LS prevents the model from becoming overfit by assigning the soft labels to ground truth data, especially when noise and ambiguity are present. This contributes to handling hard predictions and helps to prevent the wrong prediction due to the overfitting of the model.

To account for class imbalance, class weights $w_c$ are computed as the inverse of class frequency, depicted in Equation 2:

$$w_c = \frac{C \cdot n_c}{n} \qquad (2)$$

where:

· $w_c$ is the class weight for class *c*.

· *n* is the total number of samples in the dataset.

· *C* is the number of classes.

· $n_c$ is the number of samples in class *c*.

In addition to class weighting, label smoothing is applied to the ground truth labels. The smoothed label for class [21] is depicted in Equation 3:

$$y_c^{\text{smooth}(i)} = (1-\alpha) \cdot y_c^{(i)} + \frac{\alpha}{C} \quad (3)$$

where:

· $y_c^{(i)}$ is the original one-hot encoded label for class *c* in sample *i*.

· *α* is the label smoothing factor.

· *C* is the number of classes.

For each sample $i$, the loss $(\mathcal{L})$ is computed as the weighted categorical cross-entropy with label smoothing, as depicted in Equation 4:

$$\mathcal{L}^{(i)} = -\sum_{c=1}^{C} w_c \cdot y_c^{\text{smooth}(i)} \cdot \log\left(\widehat{y}_c^{(i)}\right) \quad (4)$$

where:

· $\mathcal{L}^{(i)}$ is the loss for the $i^{\text{th}}$ sample.

· $w_c$ is the class weight for class *c*.

· $y_c^{\text{smooth}(i)}$ is the smoothed label for class *c* in sample *i*.

· $\widehat{y_c^{(i)}}$ is the predicted probability for class *c* in sample *i*.

The total loss over a batch of *N* samples is the average of the per-sample losses, calculated using Equation 5:

$$\text{Loss}_{\text{batch}} = \frac{1}{N}\sum_{i=1}^{N} \mathcal{L}^{(i)} = \frac{1}{N}\sum_{i=1}^{N}\left(-\sum_{c=1}^{C} w_c \cdot y_c^{\text{smooth}(i)} \cdot \log\left(\widehat{y}_c^{(i)}\right)\right) \quad (5)$$

*Machine Learning Classifiers*

KNN is a popular, non-parametric, and supervised ML classification algorithm. KNN assigns the class label to the K-nearest patterns to the target pattern in the data space and delivers helpful information for the classification task. Initially, the algorithm examines all observation values as a single cluster, and after that, the clusters gradually merge to form new clusters. The Euclidean distance approach is widely used to find the closest neighbors (k). RF is a robust tree-based ensemble ML algorithm that makes predictions based on the voting of all the trees. RF algorithm gives the resulting output by averaging the output of multiple decision trees. Each tree in the ensemble comprises a data sample drawn from a training set with replacement, called the bootstrap sample. RF also reduces the risk of overfitting and evaluates variable importance, contributing more to the model.

## Model evaluation parameters

The performance matrices utilised to evaluate each classifier model's ability and performance output are as follows [22]:

· Accuracy measures the proportion of correct predictions out of all the predictions made by the model using the entire dataset and is computed using Equation 6.

$$Accuracy = \frac{TP+TN}{TP+TN+FP+FN} \quad (6)$$

· Precision evaluated the model's predictive capacity by estimating the proportions of true positives among all positive predictions, and its score was calculated using Equation 7.

$$Precision = \frac{TP}{TP + FP} \tag{7}$$

• Recall, also known as sensitivity or true positive rate, measures the proportion of true positive instances among all true actual positive instances, and the recall score is calculated using Equation 8.

$$Recall = \frac{TP}{TP + FN} \tag{8}$$

• F1-score is a harmonic mean of the precision and recall scores calculated using Equation 9.

$$F1 - score = \frac{2 \times (Precision \times Recall)}{Precision + Recall} \tag{9}$$

• Confusion matrix is a visualisation tool that assesses the classification model's performance in table form by comparing the predicted output against the ground truth output for the entire dataset.

In Equations 6-9, the notation depicts TP as the true positive, TN as the true negative, FP as the false positive, and FN as the false negative.

### Hardware and software

The optimised ANN was implemented in Python using the TensorFlow framework. KNN and RF models were also implemented in Python using the scikit-learn library on Jupyter Notebook. All three models were trained using a system running Windows 11, equipped with an AMD Ryzen 9 5950X processor, 64 GB of RAM, and an NVIDIA RTX 3080 Ti GPU with 12 GB of VRAM.

## Results

The representative RGB images of damaged, healthy, and diseased leaves with their corresponding spectra for the selected region of interest on the HSI leaf image for the wavelength range of 400-900 nm are shown in Figure 4.

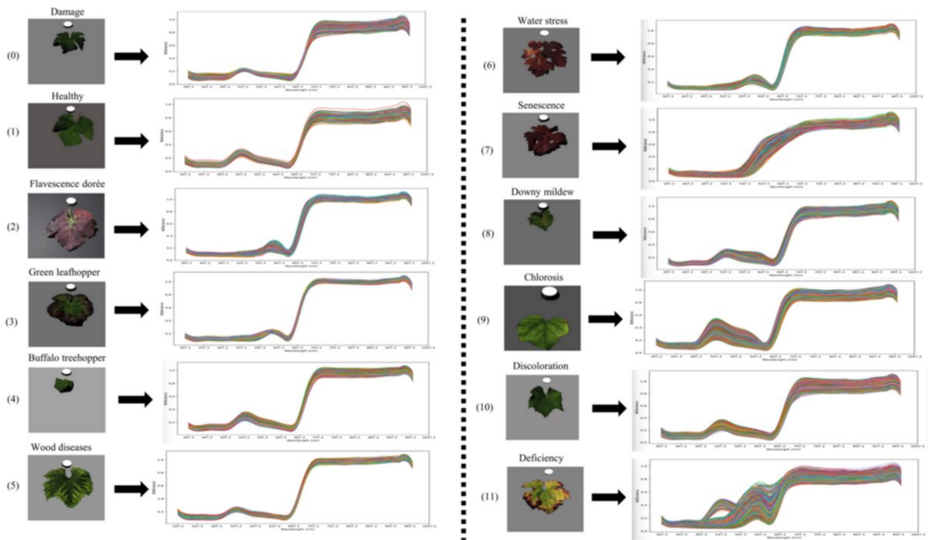


**FIGURE 4: RGB image of grapevine leaves and corresponding spectra for the VIS-NIR range (400–900 nm).**

RGB, Red, Green, and Blue; VIS-NIR, Visible-Near Infrared

The top 30 signature wavelengths (nm) identified using the LDA method with a high feature importance score are shown in Figure 5.

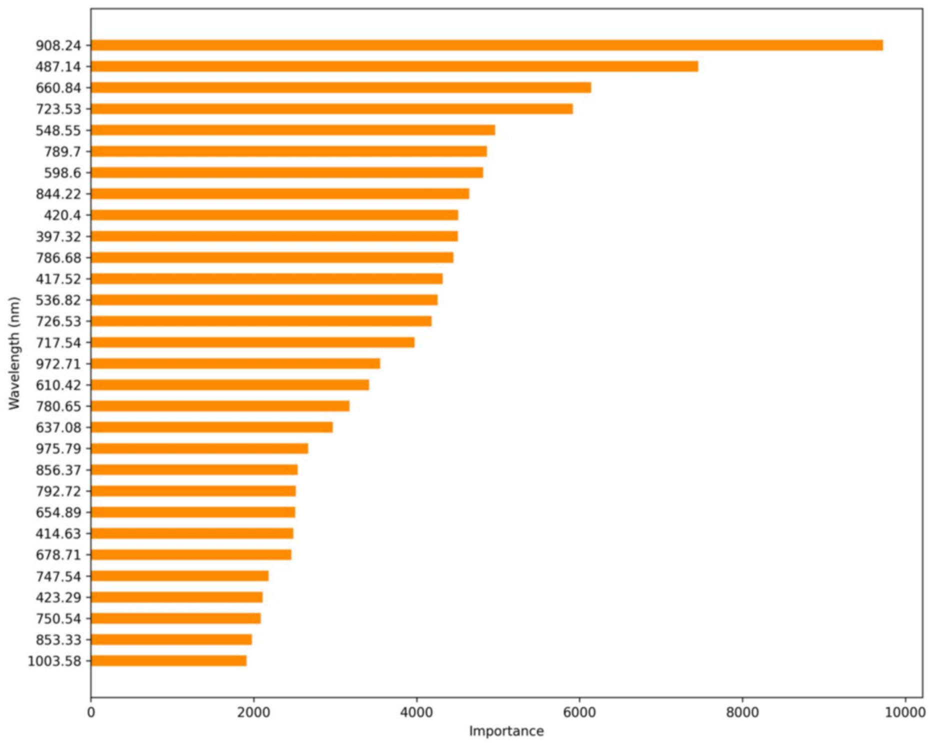


**FIGURE 5: Significant 30 features (wavelengths) obtained from the LDA model for grapevine leaves classification.**

LDA, Linear Discriminant Analysis

MCC results on Dataset-A with 10-fold CV settings and unseen Dataset-B for the grapevine leaves dataset using the optimised ANN, KNN, and RFC models for the full-range spectra (400-900 nm) are shown in Table 3.

| **Dataset-A** | | | | |
|---|---|---|---|---|
| **Model** | Accuracy (%) | Precision (%) | Recall (%) | F1-Score (%) |
| Optimised ANN | 96.37±0.26 | 96.22±0.35 | 96.68±0.25 | 96.44±0.27 |
| K-Nearest Neighbor | 86.35±0.43 | 85.31±0.33 | 85.76±0.42 | 85.50±0.35 |
| Random Forest Classifier | 86.91±0.51 | 87.87±0.44 | 85.12±0.54 | 86.37±0.45 |
| **Dataset-B** | | | | |
| Optimised ANN | 96.47 | 96.36 | 96.83 | 96.59 |
| K-Nearest Neighbor | 86.15 | 86.18 | 86.15 | 86.15 |
| Random Forest Classifier | 87.23 | 87.23 | 87.23 | 87.15 |

**TABLE 3: Comparison analysis of classifiers on Dataset-A with 10-fold cross-validation setting and unseen Dataset-B using the full-range spectra (400–900 nm) for multiclass disease classification in leaves.**

ANN, Artificial Neural Network

Later, the optimised ANN, KNN, and RF models are performed on the grapevine leaves dataset by utilising the selected 30 signature wavelengths for the MCC. The results for Dataset-A with 10-fold CV settings and unseen Dataset-B are reported in Table 4.

| Dataset-A | | | | |
|---|---|---|---|---|
| **Model** | Accuracy (%) | Precision (%) | Recall (%) | F1-Score (%) |
| Optimised ANN | 95.47±0.34 | 95.48±0.34 | 95.84±0.46 | 95.64±0.35 |
| K-Nearest Neighbor | 85.76±0.39 | 84.52±0.29 | 84.98±0.30 | 84.71±0.28 |
| Random Forest Classifier | 85.58±0.53 | 86.26±0.59 | 83.28±0.47 | 84.61±0.48 |
| **Dataset-B** | | | | |
| Optimised ANN | 95.17 | 95.05 | 95.63 | 95.32 |
| K-Nearest Neighbor | 85.77 | 85.78 | 85.77 | 85.75 |
| Random Forest Classifier | 85.83 | 85.82 | 85.83 | 85.71 |

**TABLE 4: Comparison analysis of classifiers on Dataset-A with 10-fold cross-validation setting and unseen Dataset-B using the selected 30 signature wavelengths for multiclass disease classification in leaves.**

The confusion matrix in percentage for the unseen Dataset-B utilising the optimised ANN model for the full range and the selected 30 significant wavelengths is shown in Figure 6. The confusion matrix visualises the model's performance by quantifying the accurately predicted and misclassified samples for the dataset.

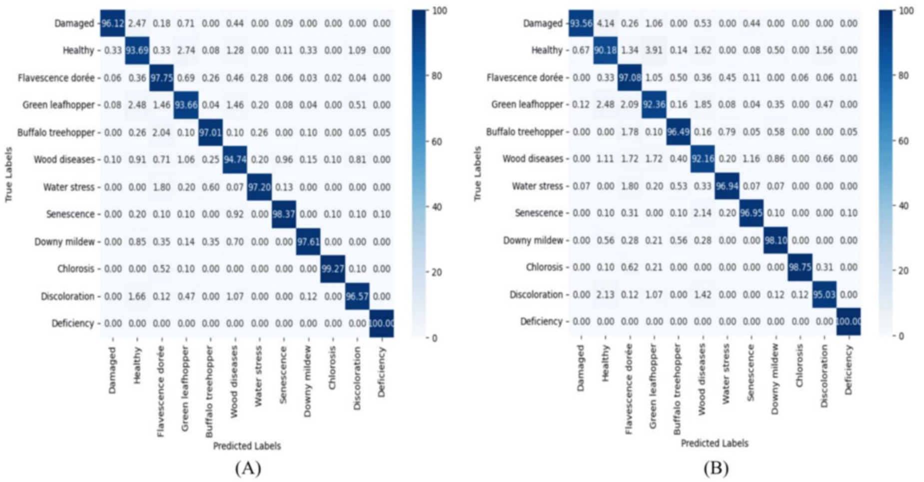


**FIGURE 6: Confusion matrix (%) for grapevine disease classification in leaves on unseen Dataset-B using the optimised ANN model. (A) Full-range spectra. (B) Selected 30 significant wavelengths.**

ANN, Artificial Neural Network

The class-wise results on Dataset-A for each fold for the grapevine leaves dataset using the proposed ANN model, evaluated using the selected 30 spectral wavelengths, are reported in Table 5.

| No. of classes | F1-score (%) | | | | | | | | | | |
|---|---|---|---|---|---|---|---|---|---|---|---|
| | Fold 1 | Fold 2 | Fold 3 | Fold 4 | Fold 5 | Fold 6 | Fold 7 | Fold 8 | Fold 9 | Fold 10 | Average performance (%) |
| Damaged | 97 | 96 | 96 | 98 | 96 | 96 | 99 | 98 | 96 | 96 | 96.80 ± 1.14 |
| Healthy | 94 | 93 | 93 | 93 | 91 | 91 | 93 | 93 | 93 | 92 | 92.60 ± 0.97 |
| Flavescence dorée | 98 | 97 | 97 | 97 | 97 | 97 | 98 | 97 | 98 | 97 | 97.30 ± 0.48 |
| Green leafhopper | 92 | 93 | 90 | 94 | 90 | 90 | 90 | 92 | 92 | 90 | 91.30 ± 1.49 |
| Buffalo treehopper | 97 | 96 | 96 | 95 | 96 | 96 | 97 | 96 | 97 | 98 | 96.40 ± 0.84 |
| Wood diseases | 93 | 93 | 90 | 93 | 91 | 90 | 92 | 91 | 94 | 92 | 91.90 ± 1.37 |
| Water stress | 97 | 98 | 97 | 95 | 97 | 97 | 97 | 97 | 96 | 97 | 96.80 ± 0.79 |
| Senescence | 97 | 97 | 95 | 97 | 97 | 96 | 97 | 97 | 98 | 97 | 96.80 ± 0.79 |
| Downy mildew | 97 | 97 | 95 | 97 | 98 | 98 | 97 | 97 | 98 | 98 | 97.20 ± 0.92 |
| Chlorosis | 99 | 100 | 100 | 100 | 99 | 100 | 100 | 98 | 99 | 100 | 99.50 ± 0.71 |
| Discolouration | 92 | 91 | 90 | 89 | 92 | 91 | 90 | 92 | 94 | 92 | 91.30 ± 1.42 |
| Deficiency | 99 | 100 | 100 | 100 | 100 | 99 | 100 | 99 | 100 | 99 | 99.60 ± 0.52 |

**TABLE 5: Class-wise performance (F1-score) for the Dataset-A for the selected 30 significant wavelengths.**

Figure 7 illustrates the loss plot of the proposed ANN model, depicting the training and test loss across 2,000 epochs for the best-performing fold.

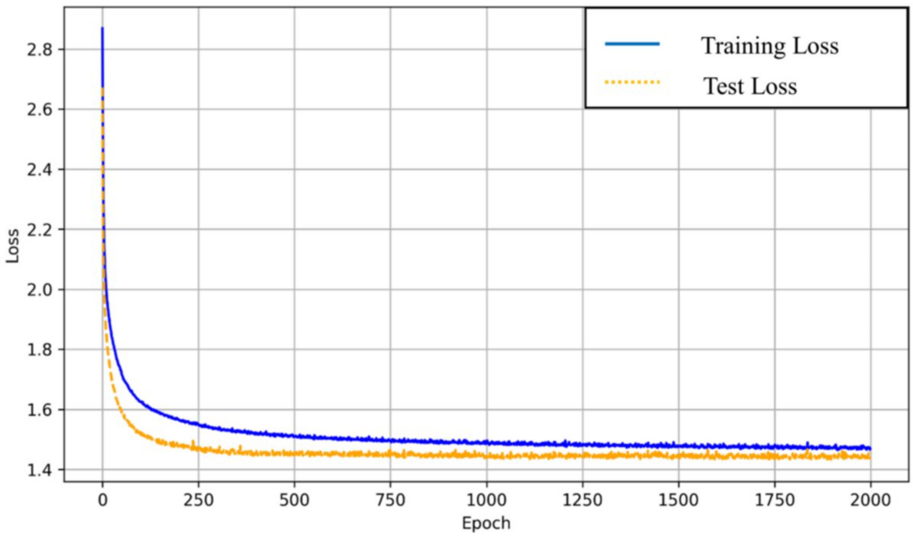


**FIGURE 7: Loss plot for the best fold.**

## Discussion

The current study develops an MCC model for classifying different kinds of diseased, damaged, and healthy leaves by utilizing optimized ANN, KNN, and RF models on the grapevine leaves' imbalanced HSI dataset. Referring to Table 1, the leaf samples for damaged, healthy, and diseased categories are very distinct in numbers. Besides that, the diseased dataset of grapevine leaves contains 10 different symptoms; among them, the samples for the flavescence dorée symptoms were the highest compared to other diseases. On the other hand, downy mildew, chlorosis, discolouration, and deficiency-affected leaves were very few. All these constraints make the dataset very challenging for the classification task. Utilizing the optimized ANN architecture by incorporating LS and class weights as the composite loss function enhances generalisation, resulting in more accurate predictions across all classes. This includes classes with fewer data points and those more similar to other classes. This approach helps create robust models that effectively address imbalanced data and challenging prediction scenarios (Figure 3). The study's outcomes corroborated that the optimized ANN model overcomes all the challenges and is accurately anticipated for the MCC task.

The study also investigated identifying the signature wavelengths relevant for grapevine leaf disease classification to reduce data redundancy. The extracted spectra from the full range (400-900 nm) were analysed via an LDA model to identify the 30 signature wavelengths via the feature importance score generated by LDA (Figure 4).

Referring to Table 3, the optimised ANN model outperformed the other classifier models for the full-range spectra. It achieved 96.37%±0.26% classification accuracy, 96.22%±0.35% precision, 96.68%±0.25% recall, and 96.44%±0.27% F1-score for Dataset-A and 96.47% accuracy, 96.36% precision, 96.83% recall, and 96.59% F1-score for Dataset-B. KNN achieved 86.35%±0.43% classification accuracy, 85.31%±0.33% precision, 85.76%±0.42% recall, and 85.50%±0.35% F1-score for Dataset-A and 86.15% accuracy, 86.18% precision, 86.15% recall, and 86.15% F1-score for Dataset-B. RF achieved 86.91%±0.51% classification accuracy, 87.87%±0.44% precision, 85.12%±0.54% recall, and 86.37%±0.45% F1-score for Dataset-A and 87.23% accuracy, 87.23% precision, 87.23% recall, and 87.15% F1-score for Dataset-B.

Later, the study experimented with optimised ANN, KNN, and RF classifiers for the signature 30 wavelengths. Referring to Table 4, optimised ANN has emerged as the best classifier and achieved 95.47%±0.34% classification accuracy, 95.48%±0.34% precision, 95.84%±0.46% recall, and 95.64%±0.35% F1-score for Dataset-A with a 10-fold CV setting and 95.17% classification accuracy, 95.05% precision, 95.63% recall, and 95.32% F1-score for unseen Dataset-B. The KNN followed as the second multi-class classifier, with 85.76%±0.39% classification accuracy, 84.52%±0.29% precision, 84.98%±0.30% recall, and 84.71%±0.28% F1-score for Dataset-A with a 10-fold CV setting and 85.77% classification accuracy, 85.78% precision, 85.77% recall, and 85.75% F1-score for unseen Dataset-B. Similarly, the RFC is the third classifier and achieved 85.58%±0.53% classification accuracy, 86.26%±0.59% precision, 83.28%±0.47% recall, and 84.61%±0.48% F1-score for Dataset-A with a 10-fold CV setting and 85.83% classification accuracy, 85.82% precision, 85.83% recall, and 85.71% F1-score for unseen Dataset-B. Table 5 shows the class-wise F1-score for the optimised ANN model that ensures robustness across imbalanced classes. Higher accuracy indicated the number of samples correctly identified among the total number of samples. Higher precision scores indicated that all the available samples were correctly identified as true positives in a one-vs-rest fashion. At the same time, a higher recall score indicated that all the available samples were correctly identified as true negatives in a one-vs-rest manner.

The evaluation matrices validated that the optimised ANN model outperformed the other classifiers (KNN and RF) for the full range as well as the selective 30 wavelengths for the grapevine leaves classification. In the case of a full-range optimised ANN, it performed 10.39% better than KNN, whereas the 9.82% better RF model on Dataset-A. The optimised ANN model performed 10.69% better than KNN, whereas the RF model performed 9.57% better than KNN on Dataset-B. Similarly, in the case of 30 significant wavelengths, optimised ANN performed 10.17% better than KNN, whereas 10.35% better than the RF model on Dataset-A. The optimised ANN model performed 9.88% better than KNN, whereas 9.81% better than RF on Dataset-B.

Furthermore, the results of the proposed ANN model for leaves classification based on the number of classes, data samples, and the used methodology are also compared with the previous state-of-the-art literature. Table 6 illustrates the comparative analysis table for the present and previous literature studies for grapevine leaves classification. There is no direct comparison available in the literature to the best of our knowledge.

| Reference | Dataset (leaves/spectra/patches) | No. of classes | Methodology | Accuracy (%) |
|---|---|---|---|---|
| Gao et al. [6] | 100/992/NA | 2 (healthy, disease) | Least squares support vector machine | 89.93 |
| Lacotte et al. [14] | 62/NA/1386 | 2 (healthy, disease) | Support vector machine | 96.00 |
| Proposed Study | 205/87065/NA | 12 (healthy, disease (10), damage) | Proposed ANN model | 95.17 |

**TABLE 6: Comparison study between the proposed ANN model and the existing models.**

ANN, Artificial Neural Network; NA, Not Available

The performance score obtained on datasets, irrespective of the full range or the 30 selected wavelengths, was observed to be closer for damage, healthy and diseased leaf classification. For instance, the difference between the performance of the best-performing optimised ANN model for the full-range spectra and the selected significant 30 wavelengths for Dataset-A and Dataset-B is 0.93% and 1.35%, respectively, in terms of accuracy. These results also underscore that utilising 30 wavelengths compared to 204 wavelengths reduces the computational cost and complexity of the data and maintains the model's high performance. The minimal accuracy drops of less than 1.5%, despite an approximately 85% reduction in spectral features, demonstrate the effectiveness of the selected wavelengths. This outcome has several important implications. First, the significant reduction in input features considerably lowers the demand for high computational systems, reduces memory usage, and speeds up the model's training and testing process. This makes the proposed approach suitable for developing low-cost HSI and MSI systems with the selected significant features. Second, reducing features reduces the system's complexity, acquisition time, and power consumption, making it suitable for real-time applications.

## Conclusions

The current study adopts a grapevine leaves hyperspectral imaging database to demonstrate the application of a multi-class classification application. The promising results showed that the proposed models accurately identify the diseased, damaged, and healthy grapevine leaves. Among all three models, the optimised ANN performed as the best classification model and achieved improved performance matrices. To the best of our knowledge, this is the first study in the literature on classifying 12 different classes of the grapevine leaves. This study also overcomes the challenges of imbalanced datasets and overfitting by incorporating the composite loss function that combines the class weights and label smoothing in the optimised ANN model. The findings of this study should inspire future research efforts to use the proposed model to develop an MSI setup by incorporating the significant features, and also use the proposed model to classify different parameters that represent the state of healthy and diseased leaves, such as chlorophyll, nutrients, nitrogen, etc.

## Additional Information

### Author Contributions

All authors have reviewed the final version to be published and agreed to be accountable for all aspects of the work.

**Concept and design:** Sujatha Narayanan Unni, Jyotisana Meena

**Critical review of the manuscript for important intellectual content:** Sujatha Narayanan Unni

**Supervision:** Sujatha Narayanan Unni

**Acquisition, analysis, or interpretation of data:** Jyotisana Meena

**Drafting of the manuscript:** Jyotisana Meena

### Disclosures

**Human subjects:** All authors have confirmed that this study did not involve human participants or tissue.
**Animal subjects:** All authors have confirmed that this study did not involve animal subjects or tissue.
**Conflicts of interest:** In compliance with the ICMJE uniform disclosure form, all authors declare the

following: **Payment/services info:** All authors have declared that no financial support was received from any organization for the submitted work. **Financial relationships:** All authors have declared that they have no financial relationships at present or within the previous three years with any organizations that might have an interest in the submitted work. **Other relationships:** All authors have declared that there are no other relationships or activities that could appear to have influenced the submitted work.

## Acknowledgements

The authors would like to thank Mr. Deepak Bajhaiya, Biophotonics Lab, IIT Madras, for insightful discussions on the algorithm optimization.

# References

1. Gatou P, Tsiara X, Spitalas A, Sioutas S, Vonitsanos G: Artificial intelligence techniques in grapevine research: A comparative study with an extensive review of datasets, diseases, and techniques evaluation. Sensors. 2024, 24:6211. 10.3390/s24196211
2. Wei Z, Jiang Y, Liu H: Optical imaging combined with artificial intelligence in plant disease detection: a comprehensive review. Spectroscopy Letters. 2025, 1-25. 10.1080/00387010.2025.2459246
3. Ahmad W, Azhar E, Anwar M, Ahmed S, Noor T: Machine learning approaches for detecting vine diseases: A comparative analysis. Journal of Informatics and Web Engineering. 2025, 4:99-110. 10.33093/jiwe.2025.4.1.8
4. Bendel N, Kicherer A, Backhaus A, et al.: Evaluating the suitability of hyper- and multispectral imaging to detect foliar symptoms of the grapevine trunk disease Esca in vineyards. Plant Methods. 2020, 16:142. 10.1186/s13007-020-00685-3
5. Ficke A, Gadoury DM, Seem RC: Ontogenic resistance and plant disease management: A case study of grape powdery mildew. Phytopathology. 2002, 92:671-675. 10.1094/phyto.2002.92.6.671
6. Gao Z, Khot LR, Naidu RA, Zhang Q: Early detection of grapevine leafroll disease in a red-berried wine grape cultivar using hyperspectral imaging. Computers and Electronics in Agriculture. 2020, 179:105807. 10.1016/j.compag.2020.105807
7. Ferentinos KP: Deep learning models for plant disease detection and diagnosis. Computers and Electronics in Agriculture. 2018, 145:311-318. 10.1016/j.compag.2018.01.009
8. Mehrubeoglu M, Orlebeck K, Zemlan MJ, Autran W: Detecting red blotch disease in grape leaves using hyperspectral imaging. Algorithms and Technologies for Multispectral, Hyperspectral, and Ultraspectral Imagery XXII. 2016, 9840:98400D. 10.1117/12.2223814
9. Yu X, Liu S, Wang C, et al.: Detection of fungal disease in citrus fruit based on hyperspectral imaging [IN PRESS]. Information Processing in Agriculture. 2025, 10.1016/j.inpa.2025.02.006
10. Junges A, Ducati J, Scalvi Lampugnani C, Almança MA: Detection of grapevine leaf stripe disease symptoms by hyperspectral sensor. Phytopathologia Mediterranea. 2018, 57:399-406. 10.14601/Phytopathol_Mediterr-22862
11. Sagar N, Suresh KP, Sridhara S, et al.: Precision detection of grapevine downy and powdery mildew diseased leaves and fruits using enhanced ResNet50 with batch normalization. Computers and Electronics in Agriculture. 2025, 232:110144. 10.1016/j.compag.2025.110144
12. Knauer U, Matros A, Petrovic T, Zanker T, Scott ES, Seiffert U: Improved classification accuracy of powdery mildew infection levels of wine grapes by spatial-spectral analysis of hyperspectral images. Plant Methods. 2017, 13:47. 10.1186/s13007-017-0198-y
13. Pérez-Roncal C, Arazuri S, Lopez-Molina C, Jarén C, Santesteban LG, López-Maestresalas A: Exploring the potential of hyperspectral imaging to detect Esca disease complex in asymptomatic grapevine leaves. Computers and Electronics in Agriculture. 2022, 196:106863. 10.1016/j.compag.2022.106863
14. Lacotte V, Peignier S, Raynal M, Demeaux I, Delmotte F, da Silva P: Spatial-spectral analysis of hyperspectral images reveals early detection of downy mildew on grapevine leaves. International Journal of Molecular Sciences. 2022, 23:10012. 10.3390/ijms231710012
15. Ryckewaert M, Héran D, Trani J-P, et al.: Hyperspectral images of grapevine leaves including healthy leaves and leaves with biotic and abiotic symptoms. Scientific Data. 2023, 10:743. 10.1038/s41597-023-02642-w
16. Schafer R: What is a Savitzky-Golay filter? [Lecture Notes]. IEEE Signal Processing Magazine. 2011, 28:111-117. 10.1109/msp.2011.941097
17. Zou J, Han Y, So S-S: Overview of artificial neural networks. Artificial Neural Networks. Methods in Molecular Biology. Livingstone DJ (ed): Humana Press, Totowa, NJ; 2008. 458:14-22. 10.1007/978-1-60327-101-1_2
18. Kramer O: K-nearest neighbors. Dimensionality Reduction with Unsupervised Nearest Neighbors. Intelligent Systems Reference Library. Springer, Berlin, Heidelberg; 2013. 51:13-23. 10.1007/978-3-642-38652-7_2
19. Cutler A, Cutler DR, Stevens JR: Random forests. Ensemble Machine Learning. Zhang C, Ma Y (ed): Springer, New York, NY; 2012. 157-175. 10.1007/978-1-4419-9326-7_5
20. Xanthopoulos P, Pardalos PM, Trafalis TB: Linear discriminant analysis. Robust Data Mining. Springer, New York, NY; 2013. 27-33. 10.1007/978-1-4419-9878-1_4
21. Zhang C-B, Jiang P-T, Hou Q, Wei Y, Han Q, Li Z, Cheng M-M: Delving deep into label smoothing. IEEE Transactions on Image Processing. 2021, 30:5984-5996. 10.1109/tip.2021.3089942
22. Meena J, Unni SN: Design and development of a low-cost hyperspectral imaging setup via a machine-learningbased approach. Engineering Research Express. 2024, 6:035236. 10.1088/2631-8695/ad76fb